

RECLAMATION

Managing Water in the West

Piezometer Plate Testing

Research and Development Office
Science and Technology Program
Final Report ST-2016-0002-01

HL-2016-08



U.S. Department of the Interior
Bureau of Reclamation
Research and Development Office

September 2016

Mission Statements

The U.S. Department of the Interior protects America's natural resources and heritage, honors our cultures and tribal communities, and supplies the energy to power our future.

The mission of the Bureau of Reclamation is to manage, develop, and protect water and related resources in an environmentally and economically sound manner in the interest of the American public.

REPORT DOCUMENTATION PAGE			Form Approved OMB No. 0704-0188	
T1. REPORT DATE September 2016		T2. REPORT TYPE Research		T3. DATES COVERED 2016
T4. TITLE AND SUBTITLE Piezometer Plate Testing			5a. CONTRACT NUMBER 16XR0680A1-RY1541RE201620002	
			5b. GRANT NUMBER	
			5c. PROGRAM ELEMENT NUMBER	
6. AUTHOR(S) J. Kubitschek and B. Heiner			5d. PROJECT NUMBER X0002	
			5e. TASK NUMBER	
			5f. WORK UNIT NUMBER 86-685600	
7. PERFORMING ORGANIZATION NAME(S) AND ADDRESS(ES) Bureau of Reclamation Technical Service Center Hydraulic Investigations and Laboratory Services PO Box 25007, Denver, CO 80225-0007			8. PERFORMING ORGANIZATION REPORT NUMBER HL-2016-08	
9. SPONSORING / MONITORING AGENCY NAME(S) AND ADDRESS(ES) Research and Development Office U.S. Department of the Interior, Bureau of Reclamation, PO Box 25007, Denver CO 80225-0007			10. SPONSOR/MONITOR'S ACRONYM(S)	
			11. SPONSOR/MONITOR'S REPORT NUMBER(S) ST-2016-0002-01	
12. DISTRIBUTION / AVAILABILITY STATEMENT Final report can be downloaded from Reclamation's website: https://www.usbr.gov/research/				
13. SUPPLEMENTARY NOTES				
14. ABSTRACT (Maximum 200 words) Piezometer plates for static pressure measurements applicable to hydroturbine performance testing were evaluated using a water tunnel test facility at Reclamation's Hydraulics Laboratory in Denver, CO. The effects of piezometer plate length and ramp transition angle (including no ramps upstream and downstream of the piezometer plate) were evaluated. The results of this study provide basic requirement for piezometer plate design to obtain reliable measurement of static pressures. The findings indicate that a 1-in-high by 14-in-long flat plate with ramped or elliptical upstream and downstream transitions is adequate to achieve accurate static pressure measurements for the range of Re_h tested (defined in terms of offset height and mean velocities ranging from 10-18 ft/s.) This study did not consider the effects of boundary curvature or secondary flow conditions (i.e., swirl) and hence applicability of results is limited to relatively long, straight penstock sections upstream of hydroturbines.				
15. SUBJECT TERMS Static pressures, piezometers, penstocks, hydroturbines, performance testing				
16. SECURITY CLASSIFICATION OF: U			17. LIMITATION OF ABSTRACT U	18. NUMBER OF PAGES 41
a. REPORT U	b. ABSTRACT U	c. THIS PAGE U		
				19b. TELEPHONE NUMBER 303-445-2148

PEER REVIEW DOCUMENTATION

Project and Document Information

Project Name Piezometer Plate Testing WOID X0002

Document Final Report

Document Author(s) Kubitschek & Heiner Document Date 9-27-2016

Peer Reviewer Josh Mortensen, PE

Review Certification

Peer Reviewer: I have reviewed the assigned items/sections(s) noted for the above document and believe them to be in accordance with the project requirements, standards of the profession, and Reclamation policy.

Reviewer *Joshua D Mortensen* Date reviewed 9/27/16
(Signature)

Disclaimer

The information provided in this report is believed to be appropriate and accurate for the specific purposes described herein, but users bear all responsibility for exercising sound engineering judgment in its application, especially to situations different from those studied. References to commercial products do not imply endorsement by the Bureau of Reclamation and may not be used for advertising or promotional purposes.

Acknowledgements

Thanks to Dave Hulse, Warren Frizell and the Hydraulics Laboratory Shop Staff (Dane Cheek, Marty Poos, Jimmy Hastings, and Jason Black) for their assistance with this project. Their efforts, particularly those of our machinist Dane Cheek, were critical to the successful completion of this project.

Cover Photo: Test facility constructed at Reclamation's Hydraulics Laboratory in Denver, Colorado.

Executive Summary

Introduction

This report summarizes the results of laboratory testing to evaluate a specific static pressure measurement method proposed for use during hydroturbine performance testing. Hydroturbine performance testing relies on accurate measurement of penstock or scroll case static pressures. Ideally, penstock static pressure measurements are acquired using standard flush-mounted piezometer taps. However, in many cases the originally installed piezometers are no longer functional or external access to the penstock at the desired location(s) is unavailable. As a means of overcoming these difficulties, plate-mounted piezometer installations on the internal surfaces of a penstock have been proposed. Such approaches inherently introduces an offset along the flow boundary which can influence local static pressures and may lead to inaccuracy.

Objectives

The objective of this project was to determine the requirements for accurate measurement of penstock static pressures using internally mounted piezometer plates, often referred to as piezoplates.

Approach

Testing was performed using a water tunnel at Reclamation's Hydraulics Laboratory in Denver, Colorado. The water tunnel test section was constructed using $\frac{3}{4}$ -in acrylic and consisted of a 5-ft-long, 10-in by 10-in square cross section that allowed for mean test section velocities up to 18 ft/s.

Various piezoplate lengths ranging from 10-inch to 2-feet with upstream and downstream 4-, 8-, 15-, and 30-degree ramped transitions as well as 3:1 elliptical transitions were tested. Static pressures were measured using 0-5 psig pressure transducers and conventional 1/8-in-diameter piezometer taps installed at 6-in streamwise stations along the top centerline of the test section. Static pressure taps were also installed at 2-in streamwise stations along the centerline of the flat portion of the piezoplate configurations. Dynamic pressures were obtained using a conventional small diameter pitot-static (Prandtl) tube connected to a 5-psid differential pressure transducer.

Conclusions

The minimum plate length of 14 inches appears adequate to achieve accurate static pressure measurements, even without upstream and downstream transitions, provided the pressure tap is located at the center of the plate. However, the addition of 15-degree ramped or 3:1 semi-elliptical transitions improves the static pressure distributions along the piezoplates without significantly increasing the piezoplate installation length. Semi-elliptical transitions have been widely used for similar applications and were also found to improve piezoplate pressure distributions comparable to that of much longer 4-degree ramp transitions. The

basic piezoplate dimensional requirements based on results presented herein include:

- A minimum piezoplate flat length of 14 inches is adequate to eliminate effects of separation and streamline curvature over the leading and trailing edges of the piezoplate provided the piezometer tap is located at the midpoint in the streamwise direction along the plate.
- Transitions including 15-degree (maximum) ramped or 3:1 elliptical are recommended for upstream and downstream offsets to minimize streamline curvature over the piezoplate.
- Piezoplate thickness should not exceed 1 inch. While it may be possible to achieve acceptable measurements with larger offsets, the upstream and downstream transitions would produce considerably longer overall piezoplate lengths.
- Although a 3/16-in weld offset at the toe of the upstream 4-degree ramp transition did not produce a measurable effect on piezoplate measurements, installation welds should be applied in a manner that lowers the disturbance profile to the extent practical.

Contents

Page

Introduction	5
Static Pressure Measurements.....	1
Hydroturbine Performance Testing.....	6
Methods	6
Experimental Setup.....	7
Instrumentation	8
Uncertainty Estimate.....	9
Results	10
Baseline Testing.....	10
Piezoplate without Ramp Transitions.....	11
8° Ramps with 10-in Plate	16
4° Ramps with 10-in Plate	18
4° Ramps with 10-in Plate and Weld Offset.....	20
4° Ramps with 2-ft Plate.....	21
15° and 30° Ramps with 2-ft Plate	23
Elliptical Transition with 2-ft Plate.....	25
Conclusions	25
Bibliography	27

Figures

Page

Figure 1. Water tunnel test section constructed at Reclamation's Hydraulics Laboratory in Denver, CO.....	3
Figure 2. Test section schematic with piezoplate dimensions (4° ramps upstream and downstream of 2-ft-long flat plate) and piezometer tap locations.	4
Figure 3. Transducer and data acquisition system setup used to measure static pressures.	4
Figure 4. Measured static pressures along top (●) and bottom (Δ) boundaries of the test section for the range of velocities tested.....	6
Figure 5. Static pressures measured along the top of the test section (●) and along the surface of the 24-in piezoplate (Δ) for the range of reference velocities tested. Piezoplate geometry is superimposed over the x-axis to schematically show extent of piezoplate.....	8
Figure 6. Pressure coefficients computed from reference static and dynamic pressures and measured local static pressures along the top of the test section and the surface of the 24-in piezoplate.	8
Figure 7. Static pressures measured along the top of the test section (●) and along the surface of the 18-in piezoplate (Δ) for the range of reference velocities tested.	9
Figure 8. Pressure coefficients computed from reference static and dynamic pressures and measured local static pressures along the top of the test section and the surface of the 18-in piezoplate.	9
Figure 9. Static pressures measured along the top of the test section (●) and along the surface of the 14-in piezoplate (Δ) for the range of reference velocities tested.	10
Figure 10. Pressure coefficients computed from reference static and dynamic pressures and measured local static pressures along the top of the test section and the surface of the 14-in piezoplate.	10
Figure 11. Static pressures measured along the top of the test section (●) and along the surface of the 10-in piezoplate (Δ) for the range of reference velocities.....	11
Figure 12. Pressure coefficients computed from reference static and dynamic pressures and measured local static pressures along the top of the test section and the surface of the 10-in piezoplate.	11
Figure 13. Dye injection with schematic representation showing upstream stagnation zone and separation over the leading edge.	12
Figure 14. Static pressures measured along the top of the test section (●) and along the surface of the 10-in piezoplate with 8° ramps (Δ) for the range of reference velocities tested.	13
Figure 15. Pressure coefficients computed from reference static and dynamic pressures and measured local static pressures along the top of the test section and the surface of the 10-in piezoplate with 8° ramps.	13

Figure 16. Photograph of modified piezoplate configuration with 4° ramps and a 10-in-long flat plate section.....	14
Figure 17. Static pressures measured along the top of the test section (●) and along the surface of the 10-in piezoplate with 4° ramps (Δ) for the range of reference velocities tested.	15
Figure 18. Pressure coefficients computed from reference static and dynamic pressures and measured local static pressures along the top of the test section and the surface of the 10-in piezoplate with 4° ramps.	15
Figure 19. Static pressures measured along the top of the test section (●) and along the surface of the 10-in piezoplate with a transverse rod at the toe of the 4° ramp (Δ) for the range of reference velocities tested.....	16
Figure 20. Pressure coefficients computed from reference static and dynamic pressures and measured local static pressures along the top of the test section and the surface of the 10-in piezoplate with a transverse rod at the toe of the 4° ramp for the range of reference velocities tested.	17
Figure 21. Dye injection with schematic representation showing flow over 3/16-in rod offset at toe of upstream 4° ramp.	17
Figure 22. Static pressures measured along the top of the test section (●) and along the surface of the 24-in piezoplate with 4° ramps (Δ) for the range of reference velocities tested.	18
Figure 23. Pressure coefficients computed from reference static and dynamic pressures and measured local static pressures along the top of the test section and the surface of the 24-in piezoplate with 4° ramps for range of test section velocities.	19
Figure 24. Static pressures measured along the top of the test section (●) and along the surface of the 24-in piezoplate with 15° ramps (Δ) for the range of reference velocities tested.	20
Figure 25. Static pressures measured along the top of the test section (●) and along the surface of the 24-in piezoplate with 30° ramps (Δ) for the range of reference velocities tested.	20
Figure 26. Static pressures measured along the top of the test section (●) and along the surface of the 2-ft-long piezoplate (Δ) for the range of reference velocities tested.	21

Glossary of Symbols

l	Length of pressure tap
d	Diameter of pressure tap
d_r	Diameter of transverse rod
h	Offset height
x	Streamwise distance along test section
u^*	Friction velocity
U_o	Reference velocity in the section
P_s	Locally measured static pressure
P_o	Reference static pressure
P_d	Reference dynamic pressure
μ	Fluid dynamic viscosity (water)
ν	Fluid kinematic viscosity
ρ	Fluid density (water)
C_p	Pressure coefficient
Re_d	Reynolds number in terms of pressure tap diameter d
Re_h	Reynolds number in terms of offset height h

Introduction

Hydroturbine performance testing relies on accurate measurement of penstock or scroll case static pressures. Ideally, penstock static pressure measurements are acquired using standard flush-mounted piezometer taps. However, in many cases the originally installed piezometers are no longer functional or external access to the penstock at the desired location(s) is unavailable. As a means of overcoming these difficulties, plate-mounted piezometer installations on the internal surfaces of a penstock have been proposed and used (Adamkowski, *et. al.*, 2006). The installation of such plates inherently introduces an offset along the flow boundary which potentially influences local static pressures and may lead to measurement inconsistencies. The primary objective of this project is to acquire laboratory data toward establishing plate-mounted piezometer (piezoplate) requirements.

Static Pressure Measurements

Static pressure gradients normal to flow boundaries are influenced primarily by streamline curvature. Measurement errors using static pressure taps are further affected by tap geometry, including tap length to hole diameter ratio l/d , and Reynolds number Re_d (defined in terms of tap diameter d and friction velocity u^*). Errors are also introduced by tap alignment (i.e., orientation of the tap centerline with respect to the flow boundary) and edge condition; the ideal construction being a perfectly perpendicular small hole with perfectly sharp edges. Neither perfect alignment nor edge condition is practically possible and some degree of associated error is unavoidable.

It is commonly accepted that errors in measured static pressures become independent of Re_d when Re_d is sufficiently large ($Re_d > 800$). This suggests that for applications involving large Re_d , static pressure measurement error can be controlled with selection of the smallest practical l/d . In general, tap diameters between 3-9 mm (1/8 – 3/8 in) with l/d values in the range of 1.5-6 are considered acceptable (ASME, 2010).

If no streamline curvature exists, static pressures along flow boundaries would be equivalent to the free stream static pressure away from the boundary. In contrast, offsets at the boundary generally alter streamlines (the degree to which is dependent on offset size and geometry) in the near field and hence change the local static pressure. Local changes in static pressure due to streamline curvature is not considered a measurement error, but instead a deviation from free stream conditions. In the most extreme cases, flow separation occurs which dramatically reduces local static pressures for some distance downstream from the point of separation to a point where the flow ‘reattaches’. For separation to occur a sufficiently large adverse pressure gradient along a boundary is necessary. Offsets into the flow, like that of a piezometer plate, can produce conditions for separation to occur, depending on geometry. For small boundary layer thicknesses relative to step or offset height, past studies (Sherry, *et. al.*, 2009) have indicated the length of the separation zone downstream of the leading edge

is weekly dependent on Re_h and typically confined in the range of $4h - 5h$, where h is the step or offset height above the boundary.

Hydroturbine Performance Testing

The discussion of static pressure measurements in the context of piezometer plate design requires some consideration for the specific application. In lieu of direct discharge measurements, measured static pressures are typically used to determine flowrates using the pressure-time method (often referred to as the Gibson method). Another common method utilizing static pressure measurements is the Winter-Kennedy method which relies on the pressure differential developed across the flow field bounded by the curved geometry of a spiral case. In both situations, accurate static pressure measurements are critical for reliable determination of hydroturbine performance.

Methods

The relevant physical parameters affecting static pressure distributions along flow boundaries with an offset, or in this case deviations from free stream pressure (P_s) downstream of an offset may be written generally as

$$\Delta P = P_s - P_o = f(U_o, h, x, \mu, \rho),$$

where P_s is the locally measured static pressure, P_o is the free stream reference static pressure, U_o is free stream reference velocity, h is the local offset height, x is the streamwise distance downstream of the offset, μ is the fluid dynamic viscosity, and ρ is the fluid density. In non-dimensional form, the local static pressure deviation can be written in terms of the pressure coefficient

$$C_p = \frac{\Delta P}{\frac{1}{2}\rho U_o^2} = \frac{P_s - P_o}{P_d}$$

where P_d is the free stream dynamic pressure. In general, the pressure coefficient may be influenced by Re_h defined here in terms of local offset height (h), free stream velocity (U_o), and kinematic viscosity ($\nu = \mu/\rho$) as

$$Re_h = \frac{U_o h}{\nu}$$

The pressure coefficient also varies, depending on flow conditions, with length ratio x/h , defined here as the coordinate streamwise distance downstream from a selected datum, normalized with step height. Measured pressures can then be used to plot C_p values as functions of x/h for various Re_h to generally describe pressure distributions.

Experimental Setup

Testing was performed using a water tunnel constructed at Reclamation's Hydraulics Laboratory in Denver, Colorado (Figure 1). Flow to the test section was supplied via 16-in schedule 40 steel pipe using a vertical turbine pump with a variable frequency controller capable of delivering a volumetric flow rate of 20 ft³/s. The water tunnel test section was constructed using ¾-in acrylic and consisted of a 5-ft-long, 10-in by 10-in square cross section that allowed for maximum mean test section velocities up to 18 ft/s while retaining a positive test section gage pressure. The bottom of the test section was designed to be removable for access to modify the test shape (in this case the piezoplate) as necessary. An upstream contraction was installed to transition from a circular to square cross section at the entrance to the test section. The internal shape of the contraction was designed to establish flow acceleration into the test section while preventing flow separation. A flow conditioner consisting of a 2.75-ft-long tube bundle and perforated plate was placed approximately 24-ft (16 diameters) upstream of the test section to reduce pump generated swirl and skewness in velocity profiles due to upstream bends. A long diffuser was installed at the downstream end for gradual pressure recovery in the transition back to the circular cross section. Finally, a knife valve was installed downstream of the diffuser to adjust back pressure at the test section as needed.

Various piezoplate test shapes were constructed including 4-, 8-, 15-, and 30-degree ramped transitions upstream and downstream of a 2-ft-long flat section with a maximum offset height of 1 in (Figure 2). In addition, shortened plates were tested in an attempt to evaluate limiting dimensions. A 3:1 elliptical transition was also considered. The entire width of the piezoplate configurations could not be tested owing to the width limitations of the test section. However, the effect of the piezoplate geometry for field installations is predominantly two-dimensional in the absence of large secondary flow structures (i.e. swirl). Laboratory testing effectively constituted a sectional representation of the piezoplate.



Figure 1. Water tunnel test section constructed at Reclamation's Hydraulics Laboratory in Denver, CO.

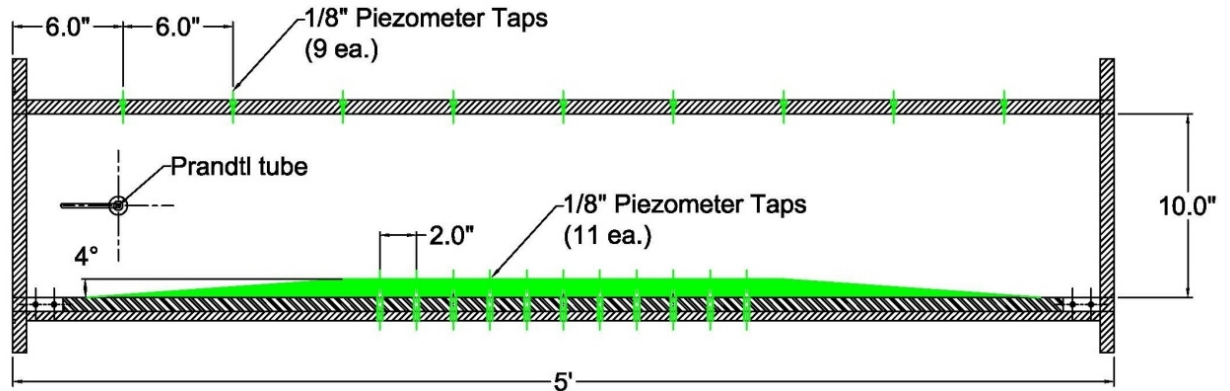


Figure 2. Test section schematic with piezoplate dimensions (4° ramps upstream and downstream of 2-ft-long flat plate) and piezometer tap locations.

Instrumentation

Test section static pressures were measured using 5-psig pressure transducers and conventional 1/8-in-diameter piezometer taps installed at 6-in streamwise stations along the top centerline of the test section. Static pressure taps were also installed at 2-in streamwise stations along the centerline of the flat portion of the piezoplate configurations. Dynamic pressures were obtained using a conventional small diameter pitot-static (Prandtl) tube connected to a 5-psid differential pressure transducer to establish reference pressures at operating set points. These data were used to determine pressure coefficients, C_p in describing the pressure distributions along the top surface of the piezoplate. The reference static pressures, P_o were obtained using the first top tap in the test section. Data were acquired at a sample rate of 100 Hz for time averaging using conventional data acquisition system hardware and associated software. Calibration checks for the pressure transducers were accomplished prior to testing using a NIST traceable secondary standard. Figure 3 shows a photograph of the pressure transducers and data acquisition setup.



Figure 3. Transducer and data acquisition system setup used to measure static pressures.

Uncertainty Estimate

The pressure transducers have a manufacturer reported NIST traceable calibration to within $\pm 0.25\%$ FS (± 0.0125 psi for 0-5 psi transducers). Contributions to the uncertainty in pressure measurements used to compute pressure coefficients can arise from known and unknown sources. Uncertainties were minimized to the extent possible using piezometer taps conforming to standard design and installation guidelines while pressure transducer elevations were held to within ± 0.030 in.

While errors from various sources cannot be eliminated, with care they can be reduced to levels necessary for meaningful results. For the purposes of this study the most significant contributions to the uncertainties in the computed pressure coefficients are expected to be due to the pressure transducers accuracy and associated measurement chain. From the pressure coefficient equation, the uncertainty can be estimated using the leading order terms in a Taylor series expansion:

$$\delta C_p \approx \pm \left\{ \left[\frac{\partial C_p}{\partial (P_s - P_o)} \delta (P_s - P_o) \right]^2 + \left(\frac{\partial C_p}{\partial P_d} \delta P_d \right)^2 \right\}^{1/2}$$

where $\delta (P_s - P_o)$ is the uncertainty associated with the difference between measured reference static pressure and measured piezometer tap pressures and δP_d is the uncertainty associated with the measured reference dynamic pressure. The partial derivatives are then given by

$$\frac{\partial C_p}{\partial (P_s - P_o)} = \frac{1}{P_d}$$

and

$$\frac{\partial C_p}{\partial P_d} = - \frac{(P_s - P_o)}{P_d^2}$$

such that

$$\delta C_p \approx \pm \left\{ \left[\frac{\delta (P_s - P_o)}{P_d} \right]^2 + \left[- \frac{(P_s - P_o) \delta P_d}{P_d^2} \right]^2 \right\}^{1/2}$$

Using the manufacturer reported accuracies for the pressure transducers, by propagation of uncertainty

$$\delta (P_s - P_o) \approx \pm [2(0.0125)^2]^{1/2} = \pm 0.018 \text{ psi} \quad \text{and} \quad \delta P_d \approx \pm 0.0125 \text{ psid}$$

With the above estimates, the uncertainties in computed pressure coefficients are obtained as $\delta C_p \approx \pm 0.02$. Random errors were confirmed to be small (within the

above estimated uncertainty) for time averaging over a duration of 5 minutes at a sample rate of 100 Hz.

Results

Baseline Testing

Baseline testing consisted of measuring static pressures along the top and bottom centerlines of the test section without a test shape installed. Measured static pressures are shown in Figure 4 along with error bars and, as expected, static pressures decrease slightly along the test section due to small pressure gradients, a result of energy losses with some boundary layer development. As test section velocity (or Re_h) increases, the pressure gradients become slightly steeper. In all cases, some pressure recovery occurs near the end of the test section due to flow deceleration in the downstream diffuser.

Reasonably good agreement (within pressure transducers accuracy) between pressures along top and bottom of the test section were obtained. Slightly larger pressures were however measured for top tap #8 (located at $x = 48$ in) in comparison with the corresponding bottom tap at the same streamwise station for all velocities tested. This suggests a small imperfection associated with installation of one or the other tap. Comparison of top and bottom pressures at the midpoint of the test section (at $x = 30$ in) show measured pressures are consistently in agreement (i.e., within the estimated uncertainty). These baseline results indicate good quality and consistency in taps installation.

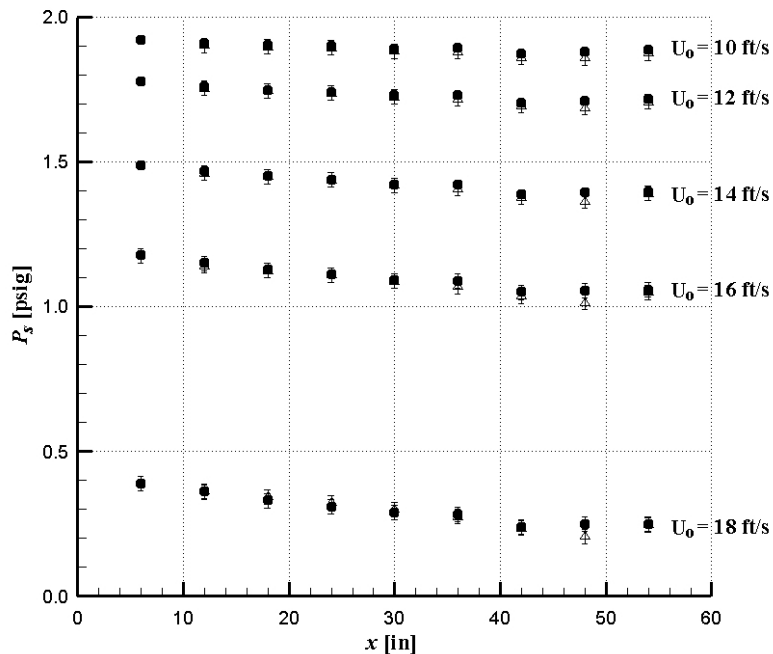


Figure 4. Measured static pressures along top (\bullet) and bottom (Δ) boundaries of the test section for the range of velocities tested.

Piezoplate without Ramp Transitions

Piezoplates of varying length were evaluated to identify static pressure measurement accuracy of a simple plate configuration without upstream and downstream transitions. Four plate lengths were tested including 24-, 18-, 14-, and 10-inches. Figure 5 shows measured static pressures along the water tunnel test section and along the top surface of the 24-in-long piezoplate. The corresponding pressure coefficients C_p are shown in Figure 6. Separation at the leading edge of the plate is evident in the negative pressure coefficients obtained along the first 4-6 inches of the plate downstream of the leading edge. The separation zone appears to reattach followed by stream line straightening as pressures recover to the test section static pressure within approximately 6-8 inches downstream of the leading edge.

Figures 7-8, 9-10, and 11-12 show results for the 18-, 14-, and 10-inch plate lengths, respectively. The separation zone is again confined to the leading 4-6 inches of the plates, consistent with past studies that indicate the separation zone length typically falls within $4h - 5h$. In most cases, pressure recovery is observed by mid-station along the plate. The exception being that pressure recovery does not occur for the 10-inch plate (Figures 11-12) as local pressures along the top surface of the plate remain below measured test section static pressures. This is a direct indication that even though reattachment occurs, streamline curvature persists over the length of the 10-inch plate resulting in reduced local static pressure distribution deviations from free stream static pressures. In contrast to the results for the 10-inch plate, measured static pressures along the 14-inch plate (Figure 9) appear to recover to test section static pressures at mid-station. It should be noted that the downstream portion of the plate is also affected by stream line curvature as evidenced by the deviations of locally measured static pressures from test section static pressures. This observation indicates that tap location upstream of the trailing edge of the piezoplate is also important.

In all case, the results for C_p verses streamwise coordinate x/h collapse well for the range of velocities (Re_h) tested. The collapse of data in nondimensional form indicates negligible Reynolds number dependence for the range of Re_h tested. Deviations from the collapse of data are shown along the separation zone. However, this is an artifact of the 0-5 psig pressure transducer limitations in measuring negative gage pressures due the inability to maintain locally positive pressures in the separation zone at the largest velocity setpoints. Had it been possible to accurately measure negative static pressures, the C_p results would be expected to collapse as shown in Figure 6. Based on previous work (Moss & Baker, 1980) the minimum C_p value should approach -1.1 which is consistent with the results obtained in Figure 6.

Figure 13 is a photograph of dye injection used to visualize the stagnation, separation, and flow reattachment phenomena. Two characteristic recirculation zones can be seen along the boundary upstream of the step near the stagnation zone and downstream on top of the step where flow separates and reattaches.

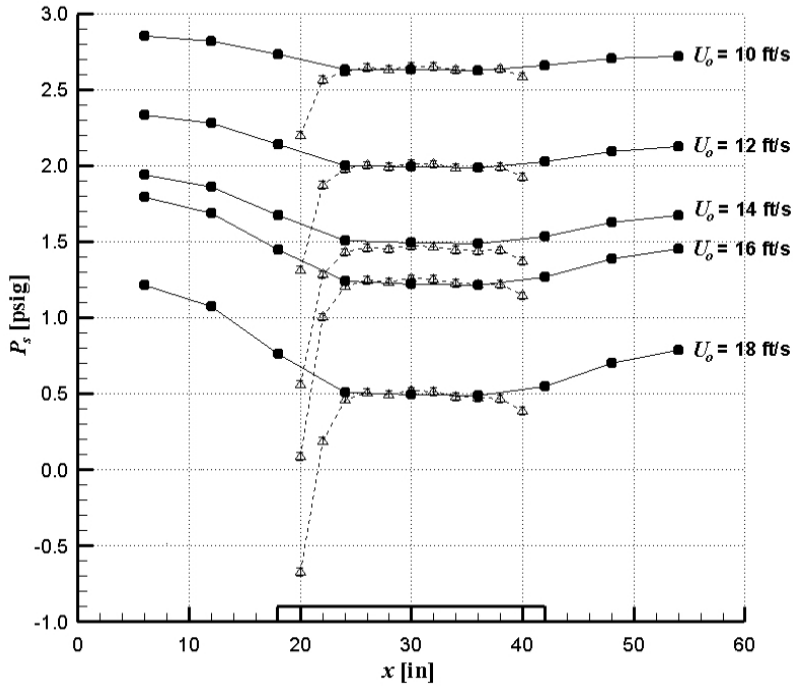


Figure 5. Static pressures measured along the top of the test section (\bullet) and along the surface of the 24-in piezoplate (Δ) for the range of reference velocities tested. Piezoplate geometry is superimposed over the x-axis to schematically show extent of piezoplate.

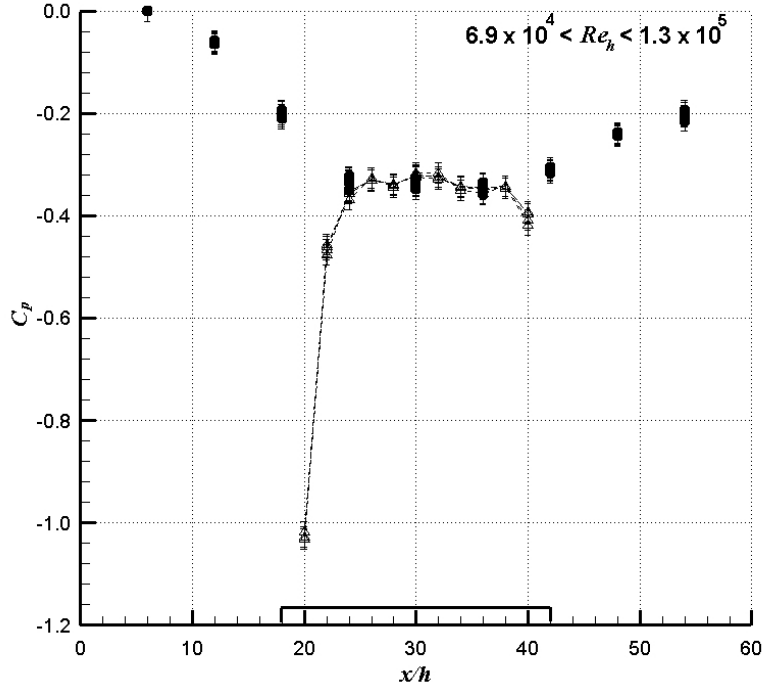


Figure 6. Pressure coefficients computed from reference static and dynamic pressures and measured local static pressures along the top of the test section and the surface of the 24-in piezoplate.

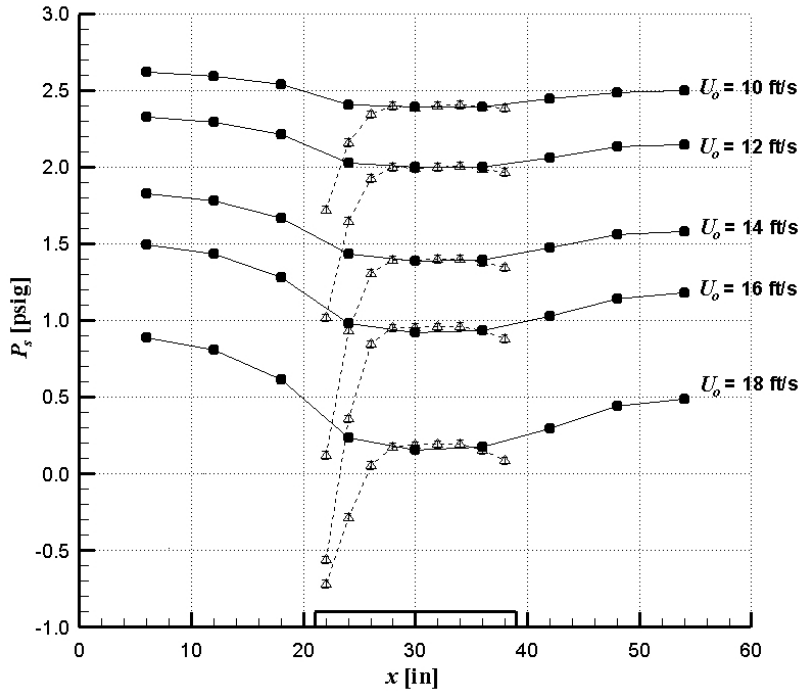


Figure 7. Static pressures measured along the top of the test section (●) and along the surface of the 18-in piezoplate (Δ) for the range of reference velocities tested.

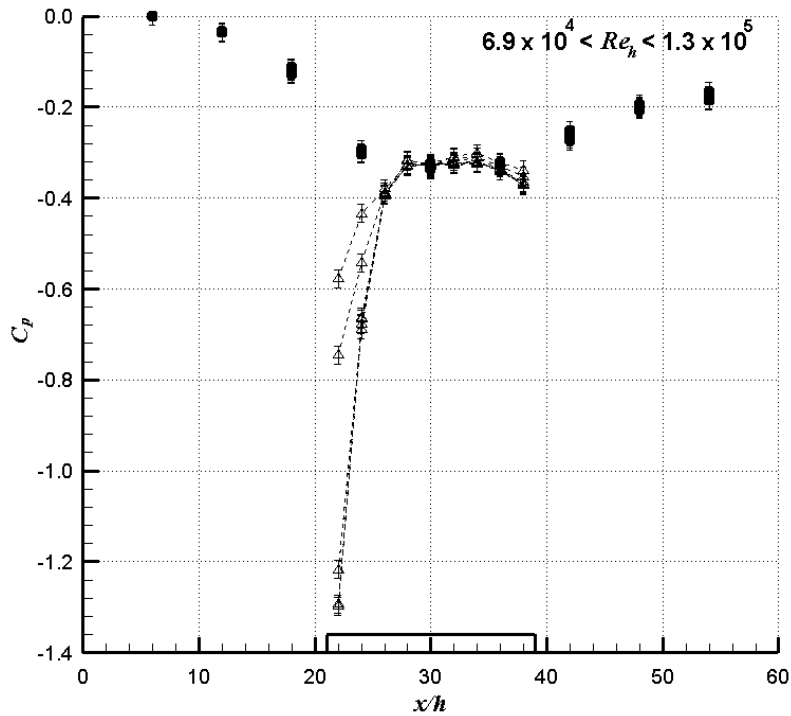


Figure 8. Pressure coefficients computed from reference static and dynamic pressures and measured local static pressures along the top of the test section and the surface of the 18-in piezoplate.

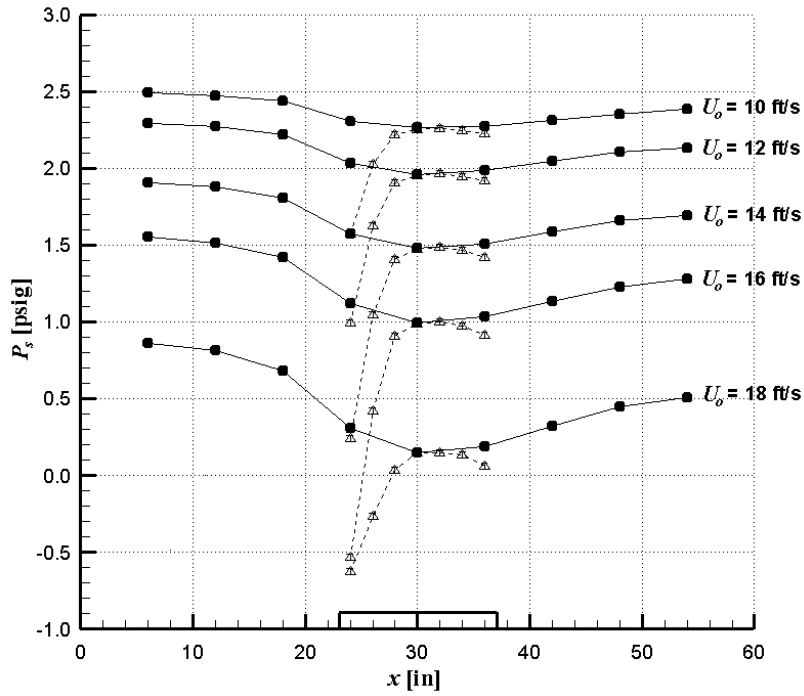


Figure 9. Static pressures measured along the top of the test section (●) and along the surface of the 14-in piezoplate (Δ) for the range of reference velocities tested.

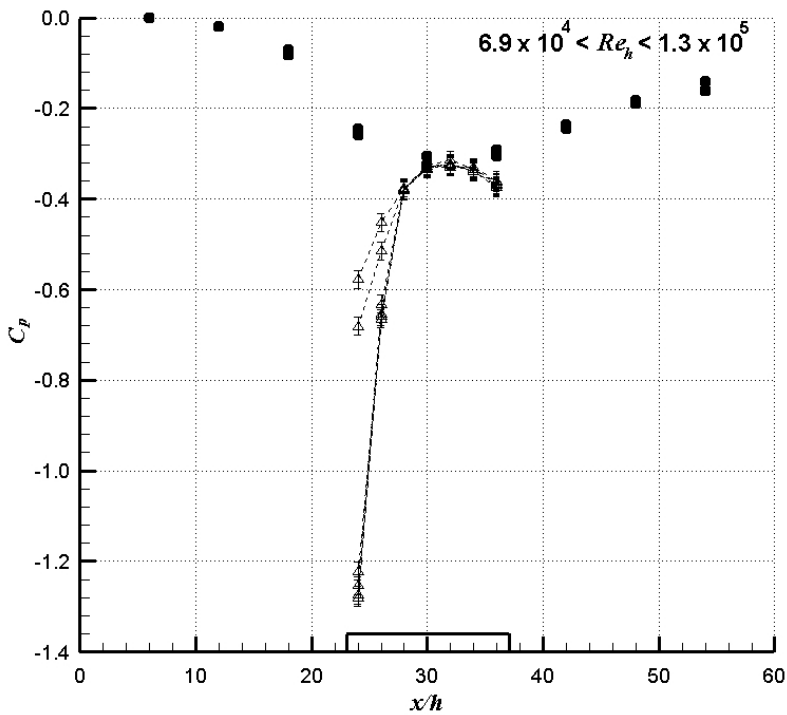


Figure 10. Pressure coefficients computed from reference static and dynamic pressures and measured local static pressures along the top of the test section and the surface of the 14-in piezoplate.

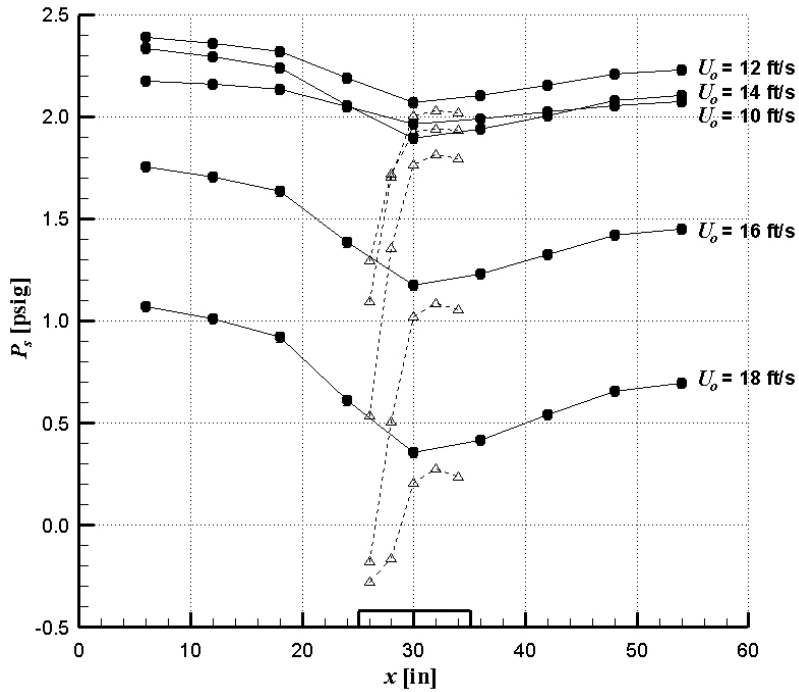


Figure 11. Static pressures measured along the top of the test section (●) and along the surface of the 10-in piezoplate (Δ) for the range of reference velocities.

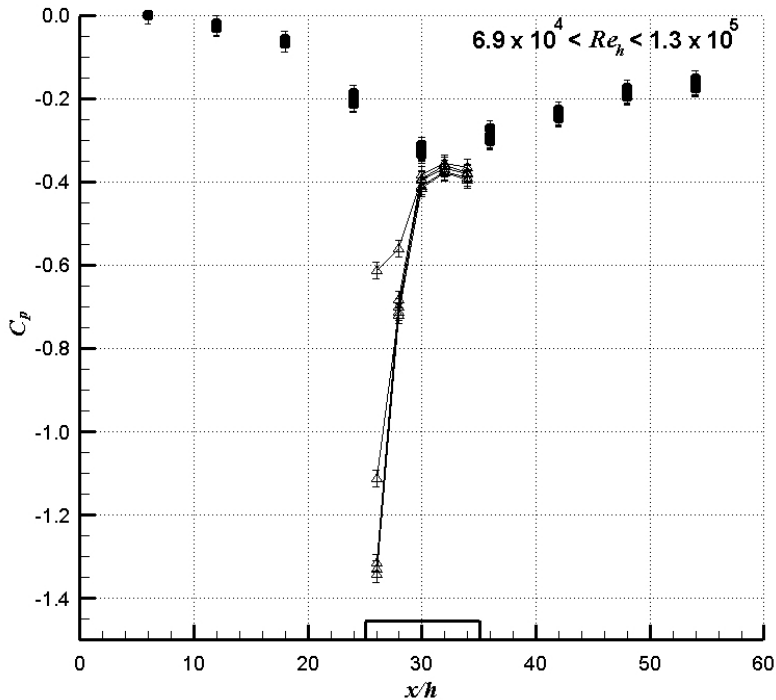


Figure 12. Pressure coefficients computed from reference static and dynamic pressures and measured local static pressures along the top of the test section and the surface of the 10-in piezoplate.

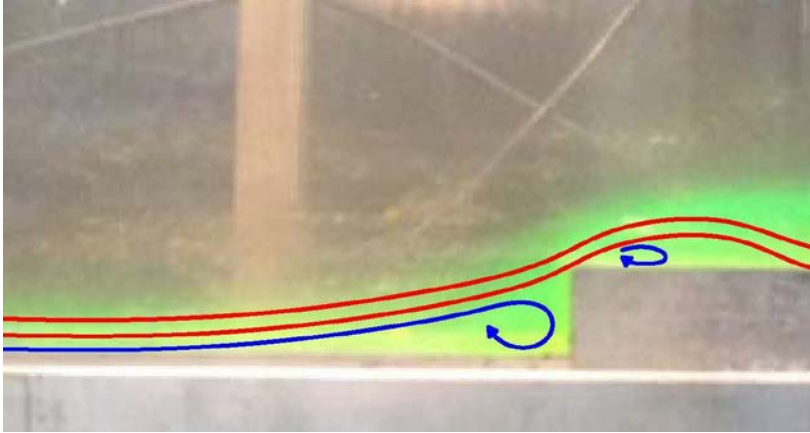


Figure 13. Dye injection with schematic representation showing upstream stagnation zone and separation over the leading edge.

8° Ramps with 10-in Plate

The 10-inch plate length was tested to determine whether transitions would improve the resulting pressure recovery. The ramp angle was set at 8 degrees with the flat length of the test shape maintained at 10 inches. Figure 14 is a plot of measured static pressures along the test section and along the top surface of the piezoplate. The static pressure distributions along the piezoplate vary significantly as compared to measurements along the top of the test section, an effect that appears to increase with test section velocity. Although separation was not observed for this ramp angle, Figure 14 shows that local pressures along the top surface of the piezoplate are lower than the test section static pressures. Furthermore, the pressure obtained from the center tap (at $x = 30$ in) on the piezoplate is measurably lower than that at the center tap on the top of the test section.

Figure 15 shows the pressure coefficients C_p versus streamwise coordinate x/h indicating lower values than free stream static pressures in the test section. The deviations obtained for this piezoplate configuration are due primarily to the streamline curvature caused by the piezoplate offset and indicate this configuration would not be expected to produce accurate static pressure measurements in a field installation.

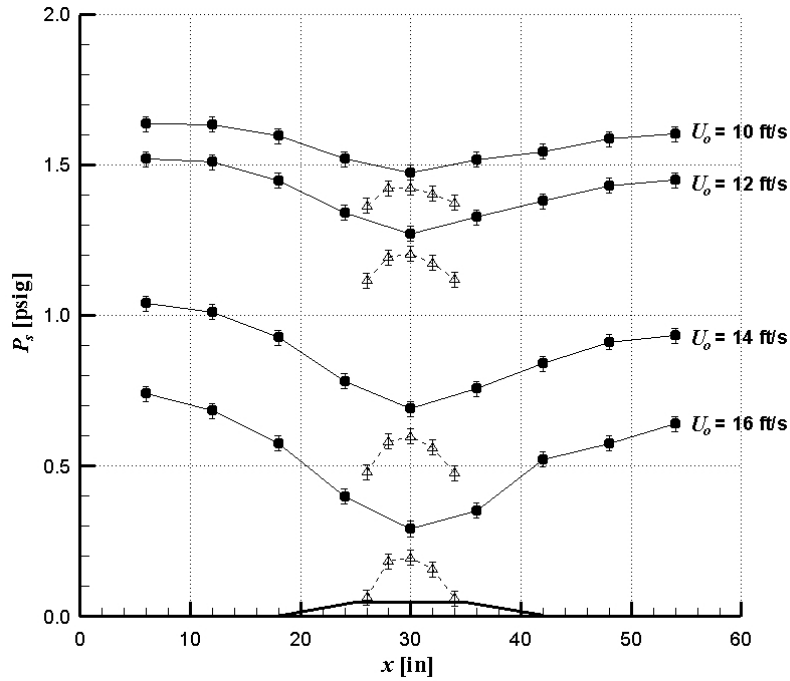


Figure 14. Static pressures measured along the top of the test section (●) and along the surface of the 10-in piezoplate with 8° ramps (Δ) for the range of reference velocities tested.

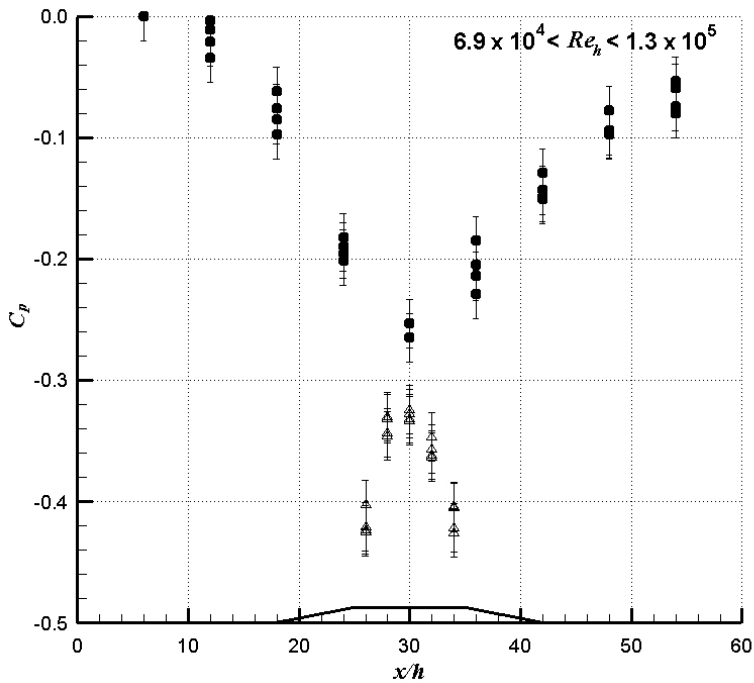


Figure 15. Pressure coefficients computed from reference static and dynamic pressures and measured local static pressures along the top of the test section and the surface of the 10-in piezoplate with 8° ramps.

4° Ramps with 10-in Plate

Upstream and downstream ramp angles were reduced to 4 degrees in a further attempt to improve the pressure distributions along the top surface of the 10-inch piezoplate. Figure 16 is a photograph of the plate configuration with 4-degree ramps as installed in the test section. Figure 17 is a plot of measured static pressures along the top of the test section and along the top surface of the piezoplate. Although the effects of separation appear to have been eliminated in comparison with Figure 11, the pressure deviations clearly increase with test section velocity with some dependence on Re_h .

Figure 18 shows normalized static pressures C_p versus streamwise coordinate x/h along the test section for the range of test section Re_h . Pressure coefficients near the center of the piezoplate (at $x/h = 30$) are clearly lower than those of the test section, particularly for the largest test section velocity, which further suggests that this piezoplate length is not sufficient even with 4-degree ramp transitions. These results indicate that excessive streamline curvature is still present over the entire length of the piezoplate. As such, this piezoplate configuration would not be expected to produce accurate static pressure measurements in a field installation.



Figure 16. Photograph of modified piezoplate configuration with 4° ramps and a 10-in-long flat plate section.

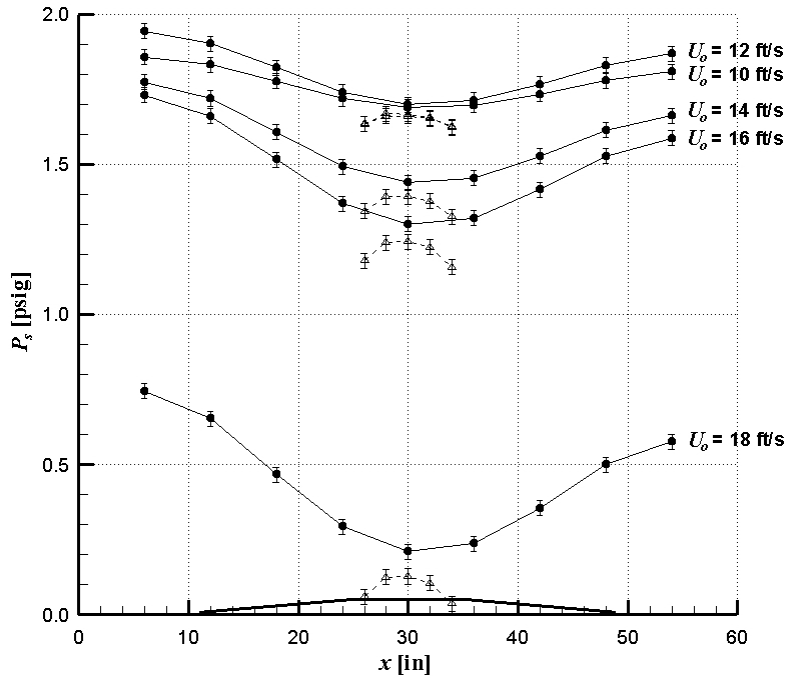


Figure 17. Static pressures measured along the top of the test section (●) and along the surface of the 10-in piezoplate with 4° ramps (Δ) for the range of reference velocities tested.

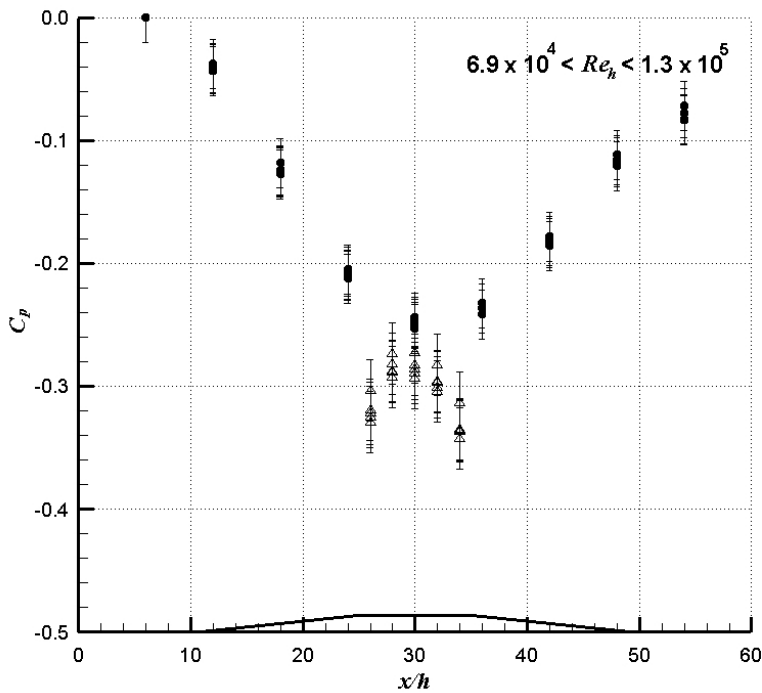


Figure 18. Pressure coefficients computed from reference static and dynamic pressures and measured local static pressures along the top of the test section and the surface of the 10-in piezoplate with 4° ramps.

4° Ramps with 10-in Plate and Weld Offset

Even though the 10-inch plate length with a 4-degree ramp did not appear sufficient, for convenience, the configuration was tested to determine whether a weld bead offset at the toe of the upstream ramp had any effect on overall plate static pressure distributions. The weld offset was represented using a 3/16-inch-diameter rod mounted in the transverse direction along the toe of the upstream ramp. Static pressures shown in Figure 19 (with the transverse rod) are similar to the results shown in Figure 17 (without the transverse rod) indicating that the transverse rod does not appear to affect the static pressures along the piezoplate. The corresponding pressure coefficients are plotted in Figure 20.

Figure 21 shows the separation zone generated by the transverse rod which is locally confined to within about $10d_r$, where d_r is the rod diameter. The presence of the ramp downstream of the rod reduces the length of the separation zone and forcing reattachment by generating a favorable pressure gradient owing to ramp geometry. Essentially the ramp effect dominates the local flow patterns as the flow transitions from ramped to flat geometry, eliminating the effect of the disturbance produced by the transverse rod. These results indicate that the transverse rod does not have a measureable effect on piezoplate pressures.

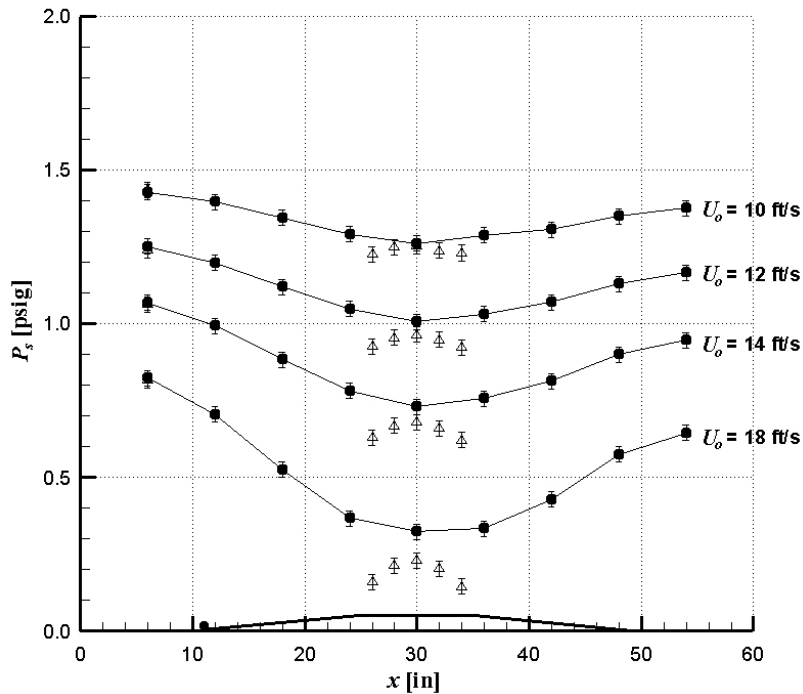


Figure 19. Static pressures measured along the top of the test section (\bullet) and along the surface of the 10-in piezoplate with a transverse rod at the toe of the 4° ramp (Δ) for the range of reference velocities tested.

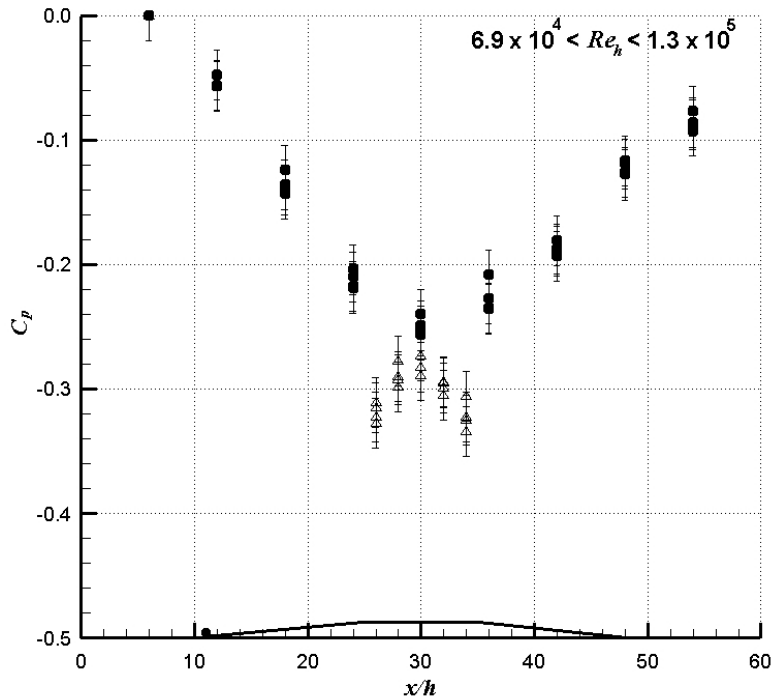


Figure 20. Pressure coefficients computed from reference static and dynamic pressures and measured local static pressures along the top of the test section and the surface of the 10-in piezoplate with a transverse rod at the toe of the 4° ramp for the range of reference velocities tested.

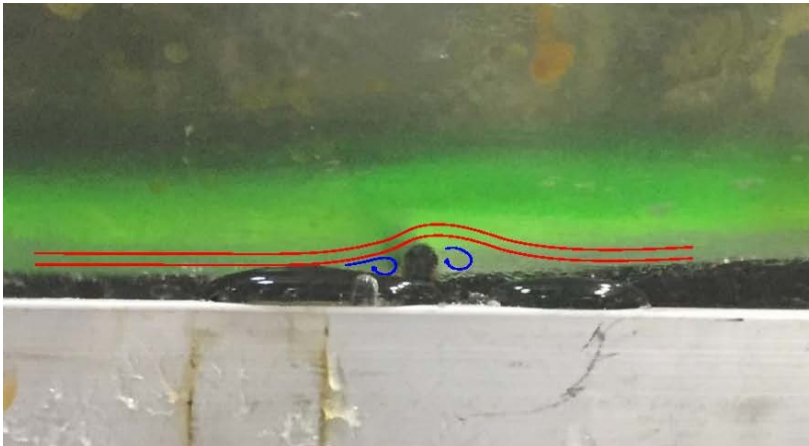


Figure 21. Dye injection with schematic representation showing flow over 3/16-in rod offset at toe of upstream 4° ramp.

4° Ramps with 2-ft Plate

The 2-ft plate configuration was also tested with 4-degree upstream and downstream ramps. Measured static pressures are plotted versus distance along the test section as Figure 22. Measured pressures along the piezoplate are in agreement with the static pressures along the top of the test section over a significant portion of the piezoplate (between approximately 26 in $< x < 34$ in). As previously discussed, lower static pressures measured at the upstream- and

downstream-most taps on the piezoplate are attributed to local stream line curvature; a result of the change in flow direction near the ramp-to-flat transition geometry.

Figure 23 shows normalized static pressures plotted as pressure coefficients C_p verses normalized streamwise distance x/h (where $h = 1$ in) along the top of the test section and along top surface of the piezoplate for the range of test section velocities (Re_h) tested. Along the center reach of the piezoplate, pressure coefficients agree (within the measurement uncertainty) suggesting that this piezoplate configuration has no measureable influence on static pressure measurements. The results again indicate that the presence of the ramp transition eliminates the separation zone as compared with Figure 5. Furthermore, if separation were present much lower C_p values would be observed, as previously shown.

Based on the results of plate testing without transitions, separation would not necessarily exclude a piezoplate arrangement from being acceptable, provided it was sufficiently long and the pressure tap location was located sufficiently far downstream of the flow reattachment.

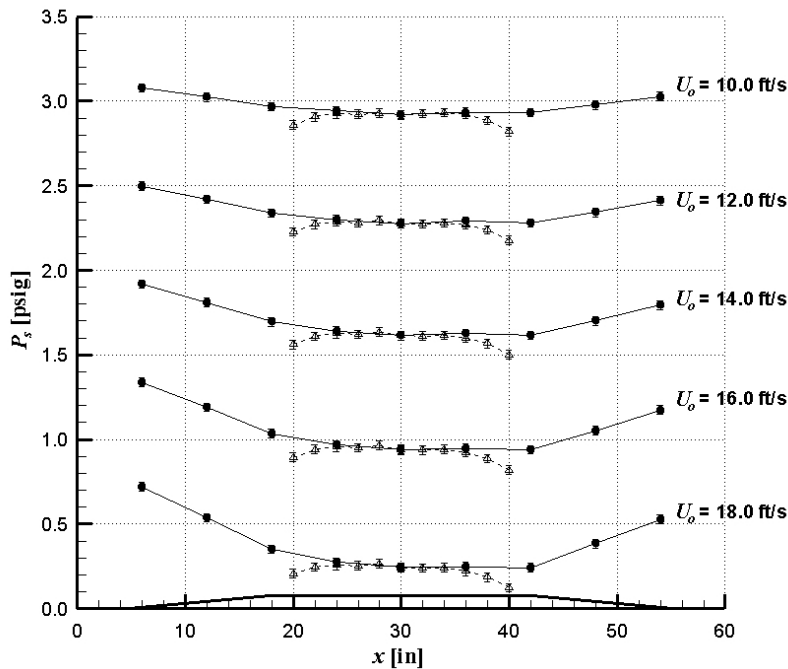


Figure 22. Static pressures measured along the top of the test section (●) and along the surface of the 24-in piezoplate with 4° ramps (Δ) for the range of reference velocities tested.

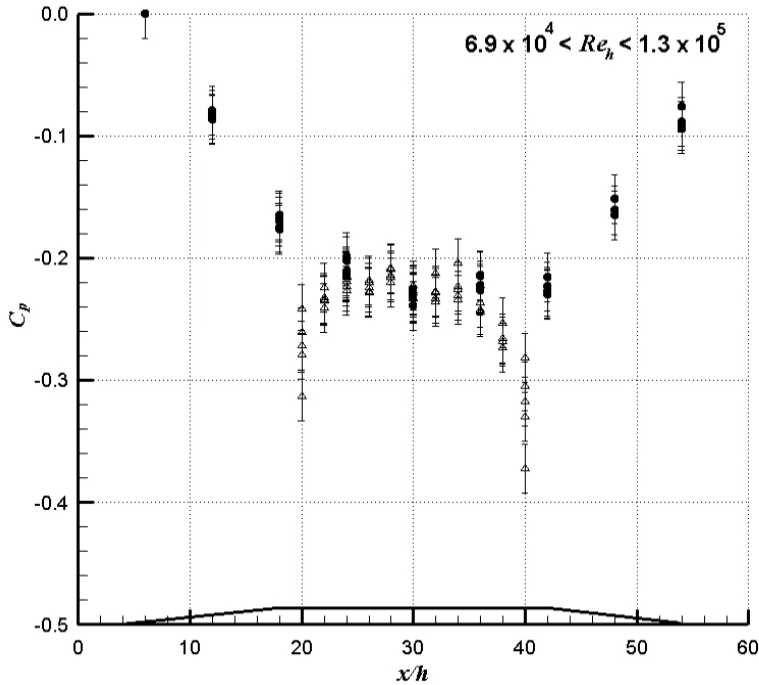


Figure 23. Pressure coefficients computed from reference static and dynamic pressures and measured local static pressures along the top of the test section and the surface of the 24-in piezoplate with 4° ramps for range of test section velocities.

15° and 30° Ramps with 2-ft Plate

To further investigate the effects of the upstream transitions, steeper 15-degree ramps were installed upstream and downstream of the 2-ft plate. Figure 24 is a plot of the measured pressures showing reduced local pressures along a greater extent of the plate downstream of the leading and trailing edges for the 15-degree configuration.

The 30-degree ramps further degrade piezoplate static pressure distributions with larger pressure reductions along the leading edge of the piezoplate (Figure 25). However, given the length of the plate (as with no transitions), acceptable static pressure measurements could be achieved with either of these configurations.

The results of the 15- and 30-degree ramp transition testing merely demonstrates that steeper ramp transitions produce lower pressures over greater extents along leading and trailing surfaces of the piezoplate. Provided the plate is sufficiently long, the effects of ramp transition angle are negligible.

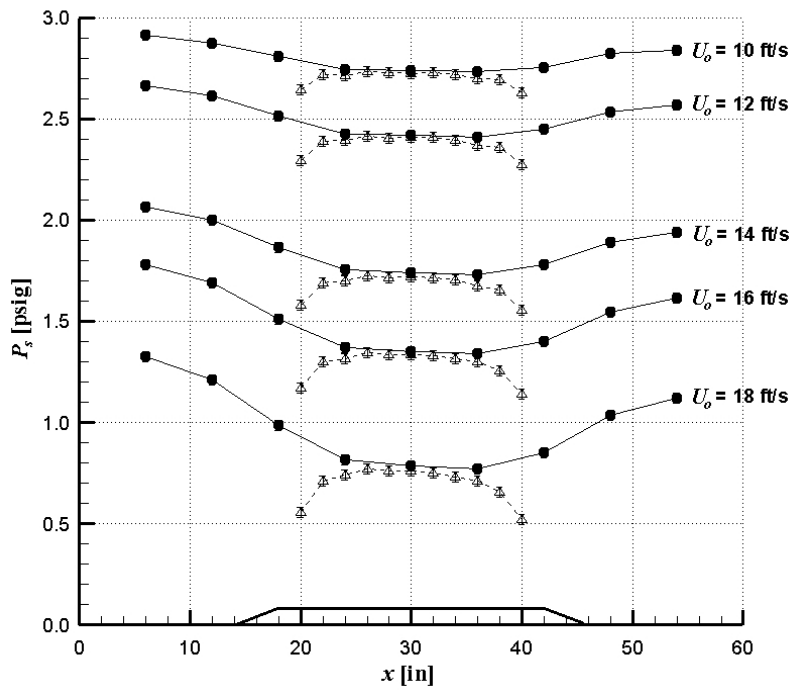


Figure 24. Static pressures measured along the top of the test section (●) and along the surface of the 24-in piezoplate with 15° ramps (Δ) for the range of reference velocities tested.

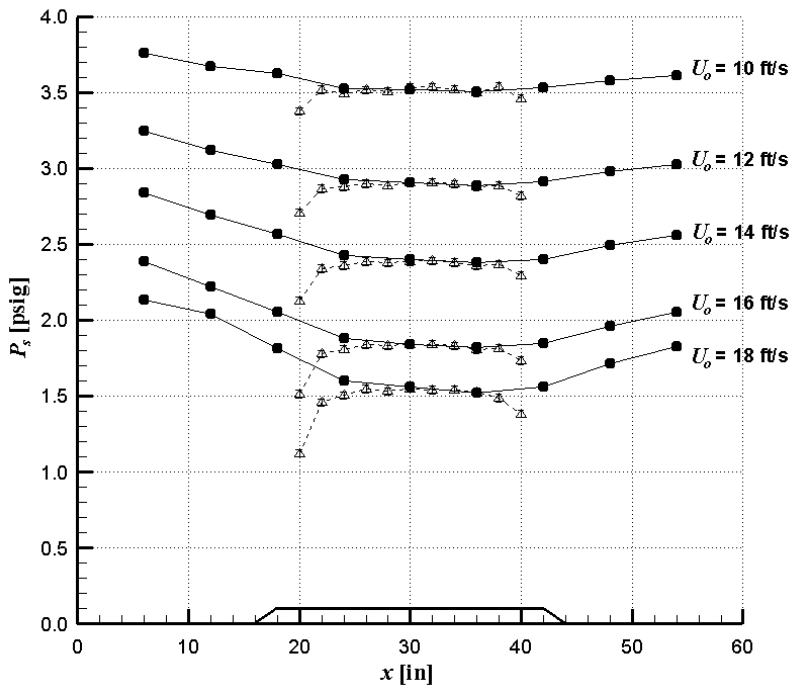


Figure 25. Static pressures measured along the top of the test section (●) and along the surface of the 24-in piezoplate with 30° ramps (Δ) for the range of reference velocities tested.

Elliptical Transition with 2-ft Plate

Final testing involved evaluating the effects of 3:1 elliptical transitions at the leading and trailing edges of the piezoplate. The measured static pressures shown in Figure 26 indicate a marked improvement in pressure distributions as compared with the 30-degree ramped transitions (Figure 25) and slight improvement over the 15-degree ramped transitions (Figure 26) with results comparable to the 4-degree ramped transitions (Figure 22).

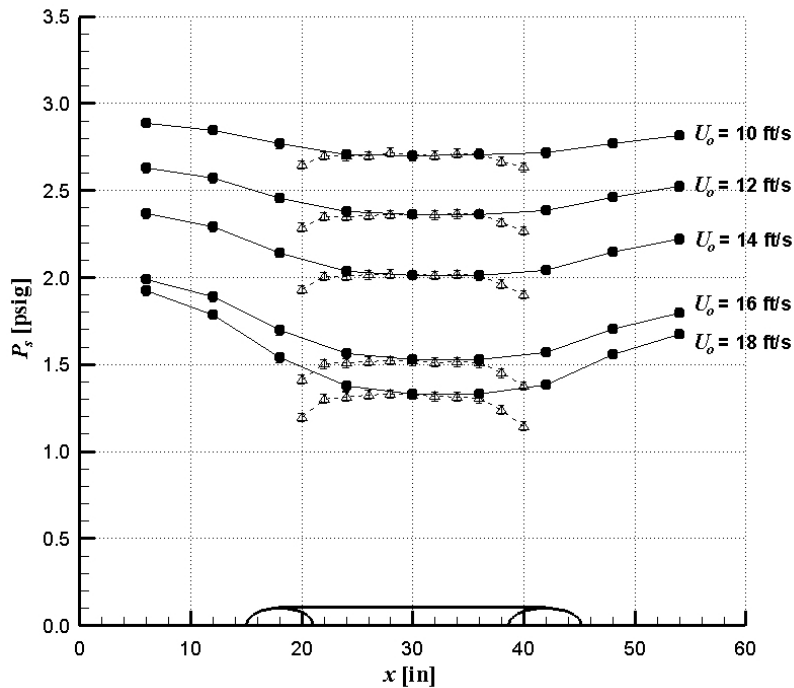


Figure 26. Static pressures measured along the top of the test section (●) and along the surface of the 2-ft-long piezoplate (Δ) for the range of reference velocities tested.

Conclusions

The piezoplate arrangements tested during this study establish requirements to achieve acceptable static pressure measurements using internally mounted piezometer plates and serve as basic guidelines to support accurate penstock static pressure measurement methods. In particular a minimum plate length of 14-in appears adequate to achieve accurate static pressure measurements, even without upstream and downstream transitions, provided the pressure tap is located at the center point along the plate. However, the addition of 15-degree ramps or 3:1 semi-elliptical transitions would improve the static pressure distributions along the piezoplates without significantly increasing the piezoplate installation length. This would allow more flexibility in the placement of the pressure tap on plates. Semi-elliptical transitions have been widely used for similar applications and were also found to improve piezoplate pressure distributions comparable to that of much longer 4-degree ramp transitions. However, semi-elliptical transitions may represent more labor-intensive machining and installation requirements.

It is important to note that this study did not account for secondary flow conditions (i.e., swirl) which can arise in many applications; namely downstream of pumps and pump-turbine equipment operated in pumping mode. Nor did this study assess boundary curvature which occurs for scroll case applications. The effects of both secondary flow patterns and boundary curvature may adversely alter piezoplate measurements resulting in deviations from free stream static pressures. In the case of swirl, the resultant free stream velocity vector would change the angle of incidence, effectively reducing the distance between the tap location and the side transition (due to the rectangular shape of the piezoplate). Similarly, boundary curvature has the potential to alter separation characteristics or the degree of streamline curvature of flow over an offset, particularly along convex surfaces. Thus, without direct testing to account for those potential effects, the applicability of these results should be limited to static pressure measurements in relatively long and straight penstocks upstream of hydroturbines operated in generating mode.

Other alternatives to the piezoplate concept may be worth consideration to provide acceptable results and reduce uncertainties associated with swirl. For example it may be possible to use conventional static pressure probes in lieu of piezometer plates. The primary advantage would be simplified installation of a lower profile, commonly accepted measurement method which may provide an alternative to the piezoplate for various applications. Notwithstanding other methods, the basic piezoplate dimensional requirements based on results presented herein include:

- A minimum piezoplate flat length of 14 inches is adequate to eliminate effects of separation and streamline curvature over the leading and trailing edges of the piezoplate provided the piezometer tap is located at the midpoint in the streamwise direction along the plate.
- Transitions including 15-degree (maximum) ramped or 3:1 elliptical are recommended for upstream and downstream offsets to minimize streamline curvature.
- Piezoplate thickness should not exceed 1 inch. While it may be possible to achieve acceptable measurements with larger offsets, upstream and downstream transitions would produce considerably longer overall piezoplate lengths.
- Although a 3/16-in weld offset at the toe of the upstream 4-degree ramp transition did not produce a measurable effect on piezoplate measurements, welds should be applied in a manner that lowers the disturbance profile to the extent practical.

Bibliography

Adamkowski, A., *et. al.*, Water turbine efficiency measurements using the Gibson Method based on special instrumentation installed inside pipelines, *6th Intl Conf Inovn Hyd Eff Meas*, Portland, OR, 2006.

ASME, Performance Test Codes: Pressure Measurement – Instruments & Apparatus Supplement, PTC 19.2-2010.

ASME, Performance Test Codes: Hydroturbines and Pump Turbines, PTC 18-2011.

Chue, S.H., Pressure probes for fluid measurements, *Prog Aerospace Sciences*, Vol. 16, No. 2, 147-243 (1975).

Camussi, R., Felli, M., Pereira, F., Aloisio, G. & Di Marco, A., Statistical properties of wall pressure fluctuations over a forward-facing step. *Phys Fluids*, 20 (2008).

Hulse, D.O., Turbine Performance Testing: Bureau of Reclamation's Experience, *HydroReview* (2008).

IEC 41: 1991, International Standard: Field Acceptance Tests to Determine the Hydraulic Performance of Hydraulic Turbines, Storage Pumps and Pump-Turbines (1991).

Largeau, J.F. & Moriniere, V., Wall pressure fluctuations and topology in separated flows over a forward-facing step, *Experiments in Fluids*, Vol. 42, p. 21-40 (2007).

McKeon, B.J. & Smits, A.J., Static pressure correction in high Reynolds number fully developed turbulent pipe flow, *Meas Sci Tech.* **13**, 1608-1614 (2002).

Moison, E., Proulx, G. & Labrecque, Y., New pressure tap design for Outardes 4 efficiency measurement after refurbishment, Report by Alstom Hydro and Hydro-Quebec (Unpublished)

Moss, W.D. & Baker, S., Re-circulating flows associated with two-dimensional steps, *Aero Quart*, p. 151-172 (1980).

Sheldon, L.H., Efficiency Testing: New Method to Determine Turbine Absolute Flow and Absolute Efficiency Data, *HydroReview* (2010).

Sherry, *et. al.*, Flow separation characterization of a forward facing step immersed in a turbulent boundary layer, *6th Intl Symp on Turbulence & Shear Flow Phenomena*, Seoul, Korea, 22-24 June (2009).

Piezometer Plate Testing

Song, S., Degraaff D.B., & Eaton, J.K., Experimental study of separating, reattaching, and redeveloping flow over a smoothly contoured ramp, *Int J Heat & Fluid Flow*, 21, p.512-519 (2000).